JACS
JOURNAL OF THE AMERICAN CHEMICAL SOCIETY
pubs.acs.org/JACS

Article

Chirality-Promoted Chemical Ligation and Reverse Transcription of *Acyclic* Threoninol Nucleic Acid

Hikari Okita, Keiji Murayama,* and Hiroyuki Asanuma*

Cite This: *J. Am. Chem. Soc.* 2025, 147, 17967−17974

Read Online

ACCESS | Metrics & More | Article Recommendations | Supporting Information

ABSTRACT: The building blocks of current life on Earth are chiral compounds, such as 2'-deoxy-D-ribose of DNA and L-amino acids with homochirality, which play an important role in various biological reactions. We investigated the effect of chirality on the template-directed chemical synthesis of nucleic acids as a model for primitive replication of genetic materials in the absence of enzymes. The efficiency of the template-directed chemical ligation of two *acyclic* nucleic acids, achiral serinol nucleic acid (SNA) and chiral *acyclic* L-threoninol nucleic acid (L-*a*TNA), induced by *N*-cyanoimidazole and a divalent metal cation, was evaluated. The chemical ligation of SNA fragments on an SNA template was much slower than the ligation of L-*a*TNA fragments on an L-*a*TNA template. Examination of L-*a*TNA and SNA heteroligation and the effects of chimeric template strands revealed the crucial importance of L-*a*TNA chirality, which induces helical propagation and fixes the local conformation of the reactive phosphate group for effective chemical ligation. DNA and RNA templates also enhanced the ligation of SNA and L-*a*TNA fragments. "Reverse transcription" from template RNA to L-*a*TNA was also demonstrated. Our findings show that scaffold chirality is crucial for chemical replication and reverse transcription in XNA-based systems. Furthermore, the reverse transcription from RNA to L-*a*TNA will find applications in XNA-based in vitro selection, the creation of artificial life, and nanotechnologies.

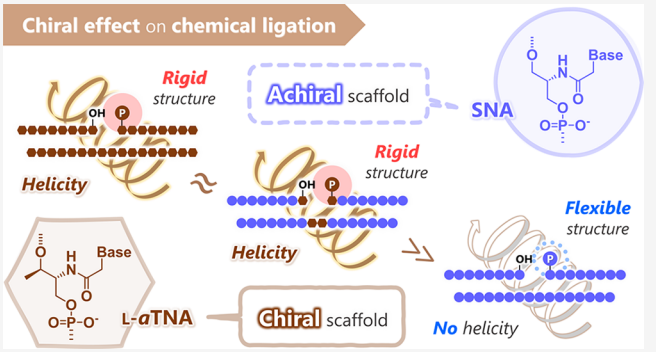

INTRODUCTION

Many of the components of living systems are chiral. The heterogeneity of the "primordial soup" resulted in homochiral macromolecules, such as D-DNA, D-RNA, and proteins composed of L-amino acids.[1,2] Hypotheses have been proposed to explain the evolution of selection for homochirality,[3] and the role of chirality and the reason why specific chirality was selected during evolution remain unclear. Moreover, the helicity derived from chiral scaffolds could affect the formation of higher-order structures, such as right-handed DNA duplexes, G-quadruplexes, RNA secondary structures, and α-helices of proteins.

Chirality is also important for nonenzymatic template-directed elongation, which is a strong candidate for the prebiotic replication system, as shown by studies on non-enzymatic strand synthesis of DNA, RNA, and xeno nucleic acid (XNA) oligomers.[1,4] Orgel, Szostak, Richert, and co-workers have established the foundations of the chemical ligation method and analyzed its detailed mechanism.[5] Most of these studies have focused on chiral specificity or selectivity rather than the impact of chirality itself because almost all XNAs have chiral scaffolds.[6] Some achiral nucleic acids were proposed as a possible pre-RNA molecule; however, these XNAs were too flexible to form a duplex.[7] One exception, peptide nucleic acid (PNA), is composed of an achiral scaffold.[8] Orgel and co-workers demonstrated template-directed elongation of PNA strands on DNA and RNA templates and RNA elongation on a PNA template,[9] and Liu et al. reported sequential ligation of PNA fragments on a DNA template.[10] To the best of our knowledge, a primer extension reaction using only PNA has not yet been reported. PNA synthesis on a PNA template has only been achieved using relatively long fragments or a base-filling reaction.[11] Very recently, Winssinger et al. demonstrated PNA elongation on a PNA template by chemical ligation; however, it needed chiral serine modification.[12] These results imply that the strand elongation of an achiral XNA is significantly inefficient compared to a chiral XNA[13]; however, this has not been demonstrated. One challenge with performing studies using achiral PNA is that it is difficult to distinguish the effects of chirality from the effects of large structural differences between DNA and PNA.

Received: February 20, 2025
Revised: April 8, 2025
Accepted: April 10, 2025
Published: April 17, 2025

https://doi.org/10.1021/jacs.5c03128
J. Am. Chem. Soc. 2025, 147, 17967−17974

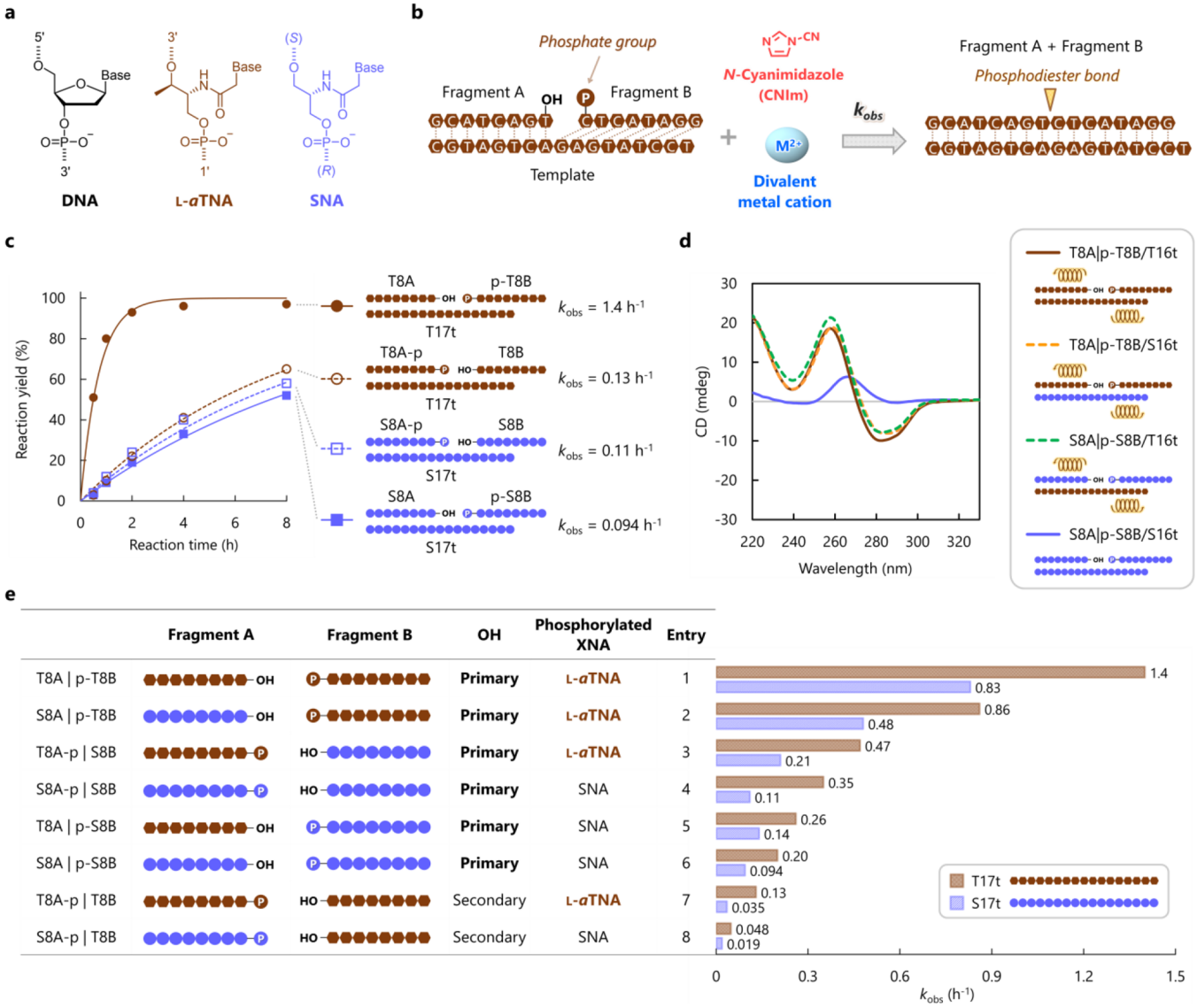

Figure 1. (a) Chemical structures of DNA, L-*a*TNA, and SNA. (b) Chemical ligation system driven by CNIm and a divalent metal cation and sequences used for the reaction. (c) Reaction rates of chemical ligations with four homofragment pairs (T8A|p-T8B/T17t, T8A-p|T8B/T17t, S8A|p-S8B/S17t, and S8A-p|S8B/S17t). Brown hexagons and blue circles indicate L-*a*TNA and SNA monomers, respectively. All sequences are listed in Table S1. (d) CD spectra of homo- and heteroduplexes formed between L-*a*TNA and SNA strands in solution containing Mn^{2+}. Conditions: 2.0 μM fragments/template, 100 mM NaCl, and 20 mM $MnCl_2$. (e) Values of k_{obs}s for homo- and heterochemical ligations of 8-mer L-*a*TNA and SNA fragments on 17-mer L-*a*TNA and SNA templates in the presence of CNIm and Mn^{2+}. Brown and blue bars show L-*a*TNA and SNA templates, respectively. Reaction conditions: 0.9 μM T8A, T8A-p, S8A, or S8A-p, 1.1 μM p-T8B, T8B, p-S8B, or S8B, 1.0 μM T17t or S17t, 100 mM NaCl, 20 mM $MnCl_2$, 20 mM CNIm, 4 °C. All k_{obs}s were calculated based on linearized plots of $-\ln([\text{Fragment A}]/[\text{Fragment A}]_0)$ as a pseudo-first-order reaction.

Herein, we evaluated the effects of chirality of the template on chemical ligation and primer extension. For this purpose, we used two acyclic XNAs, chiral *acyclic* L-threoninol nucleic acid (L-*a*TNA)[14] and achiral serinol nucleic acid (SNA); the two scaffolds differ only by a methyl group that is present on L-*a*TNA but not on SNA[15] (Figure 1a). The SNA homo oligomer has no helical preference, whereas L-*a*TNA has right-handed helicity. L-*a*TNA cross-pairs with DNA, RNA, and L-*a*TNA.[14−16] SNA forms highly stable SNA/SNA homoduplexes and cross-hybridizes with L-*a*TNA, DNA, and RNA. Due to the achiral nature of a serinol scaffold, SNA can also cross-pair with D-*a*TNA, L-DNA, and L-RNA.[16,17]

Previously, we demonstrated nonenzymatic primer extension of L-*a*TNA using chemical ligation in the presence of *N*-cyanoimidazole (CNIm) and a divalent metal cation (Figure S1).[18−20] We found that the chemical ligation of L-*a*TNA was more efficient and rapid than the ligation of DNA due to stabilization of the optimal conformation of the 3′ phosphate at the nick site and high nucleophilicity of the primary hydroxyl group.

Because SNA and L-*a*TNA have similar structural and chemical properties, studies of these two XNAs allowed us to assess the effect of chirality on nonenzymatic template-directed ligation. We demonstrated that the helicity induced by chiral L-*a*TNA remarkably increased the efficiency of chemical ligation and the primer extension compared to the achiral SNA scaffold by helical propagation and optimized local conformation around reactive phosphate. We also achieved the

https://doi.org/10.1021/jacs.5c03128
J. Am. Chem. Soc. 2025, 147, 17967−17974

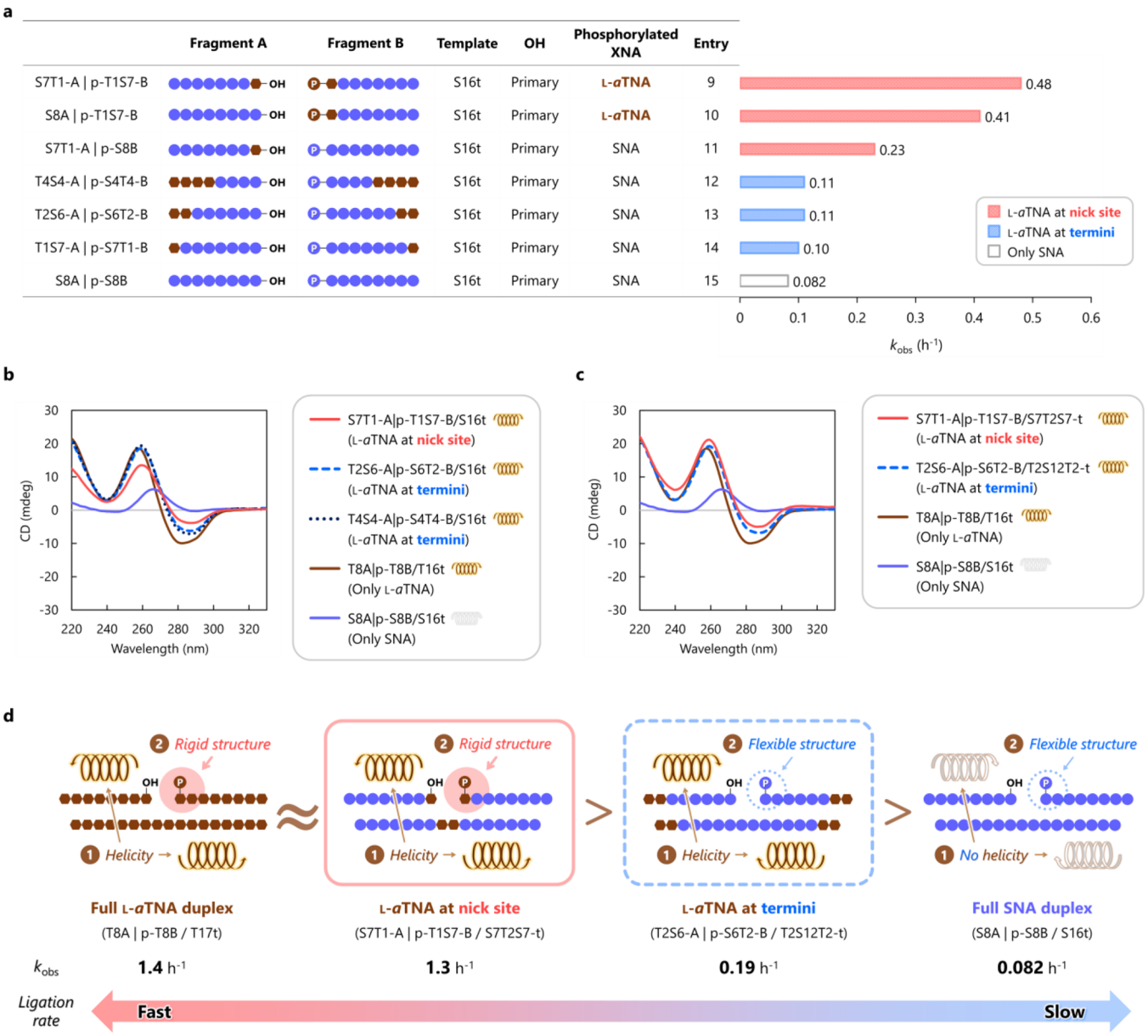

Figure 2. (a) Values of k_{obs} for chemical ligation reactions of 8-mer L-*a*TNA-SNA chimeric fragments on a 16-mer SNA template in the presence of CNIm and Mn^{2+}. (b,c) CD spectra of duplexes formed between L-*a*TNA-SNA chimeric fragments and (b) SNA template and (c) L-*a*TNA-SNA chimeric template. Conditions: 2.0 μM fragments/template, 100 mM NaCl, 20 mM $MnCl_2$. Sequences are listed in Table S1. (d) Schematic of chemical ligation of L-*a*TNA-SNA chimeric strands and effects of helicity and the local structure of phosphate on the ligation efficiency. Brown hexagons and blue circles indicate L-*a*TNA and SNA monomers, respectively. Reaction conditions: 0.9 μM fragment A, 1.1 μM fragment B, 1.0 μM template, 100 mM NaCl, 20 mM $MnCl_2$, 20 mM CNIm, and 4 °C.

chemical primer extension of L-*a*TNA with random L-*a*TNA trimers on an RNA template. These results provide insights into the importance of chirality in novel XNA-based life and partially in the primitive life system.

RESULTS AND DISCUSSION

Importance of Chirality in Chemical Ligation. To investigate the effect of chirality on chemical ligation, we first evaluated the ligation rates of SNA compared to those of L-*a*TNA. We prepared fluorescently labeled 8-mer SNA fragments S8A and S8A-p and 8-mer SNA fragments S8B and p-S8B (Figure 1b,c and Table S1). S8A-p and p-S8B were phosphorylated at the (*R*)- and (*S*)-termini, respectively. A 17-mer template (S17t) was used instead of a fully matched 16-mer template because S17t can be used in common for ligation and primer extension experiments. The use of 16-mer and 17-mer templates resulted in similar reaction rates for ligation of 8-mer fragments (Figure S2 and Table S2). We performed the chemical ligation of SNA in the presence of CNIm and Mn^{2+} at 4 °C and calculated reaction rate constants (k_{obs}s) by assuming pseudo-first-order reactions. The k_{obs} values of SNA ligation were 0.094 and 0.11 h^{-1} for S8Alp-S8B/S17t and S8A-plS8B/S17t, respectively (Figures 1c and S2). Although the reaction rate of L-*a*TNA ligation strongly depended on which strand was phosphorylated (k_{obs} = 1.4 h^{-1} for T8Alp-T8B/T17t, 0.13 h^{-1} for T8A-plT8B/T17t), the symmetric structure of the SNA resulted in almost the same k_{obs} values regardless of the direction (Figures 1c and S3). Importantly, SNA ligation was

https://doi.org/10.1021/jacs.5c03128
J. Am. Chem. Soc. 2025, 147, 17967−17974

over 12 times slower than the ligation of T8A to p-T8B on the T17t template. The thermal melting temperatures (T_ms) of the SNA and L-*a*TNA duplexes (T_ms > 44 °C, Table S3) were considerably higher than the reaction temperature (4 °C); therefore, fragments form stable duplexes with the templates. In the chemical ligation reactions, the nucleophilicity of the hydroxyl group at the nick site is primarily responsible for the ligation efficiency.[18,19,21] Nevertheless, the ligation efficiency of SNA, which has a primary hydroxyl group, was lower than that of L-*a*TNA, which has a less reactive secondary hydroxyl group (T8A-p|T8B/T17t) (Figure 1c). The low efficiency of the chemical ligation of SNA did not allow nonenzymatic primer extension using a random pool of SNA trimers (Figure S4). We hypothesize that the helicity of the duplex induced by the chiral threoninol scaffold increased the k_{obs} on the chemical ligation.

Circular dichroism (CD) spectra of the L-*a*TNA duplex are characteristic of right-handed helicity, whereas the induced CD of the SNA duplex was weak due to its achiral and flexible nature (Figure 1d), as previously described.[14,15] To confirm the effect of helicity on chemical ligation, we evaluated the chemical ligation of L-*a*TNA/SNA heteroduplexes (Figures 1e, S5, and Table S2). The CD spectra of S8Alp-S8B/T17t and T8Alp-T8B/S17t were almost the same as that of the L-*a*TNA/L-*a*TNA duplex, indicating that the L-*a*TNA/SNA heteroduplexes have the same right-handed helicity as the L-*a*TNA/L-*a*TNA homoduplex (Figure 1d). The ligation rates of SNA fragments on the L-*a*TNA template (S8Alp-S8B/T17t, k_{obs} = 0.20 h^{-1}) and those of L-*a*TNA fragments on the SNA template (T8Alp-T8B/S17t, k_{obs} = 0.83 h^{-1}) were considerably higher than those of SNA fragments on the SNA template (S8Alp-S8B/S17t, k_{obs} = 0.094 h^{-1}) (Figure 1e, entries 1 and 6). Thus, the L-*a*TNA strand induced the SNA to form a right-handed helix that facilitated rapid ligation.

We also investigated the ligation reactions that generate L-*a*TNA-SNA chimeric products. For all fragment pairs, the ligation rates on the L-*a*TNA template, T17t, were higher than those on the SNA template, S17t. When the secondary OH was a nucleophile, k_{obs} was lower (Figure 1e, entries 7 and 8), indicating that the reduced nucleophilicity severely lowered the reaction efficiency, as previously demonstrated.[18,19,21] Interestingly, the k_{obs}s of the phosphorylated L-*a*TNA fragments were larger than those of phosphorylated SNA fragments (Figure 1e, entries 1−6). We hypothesize that the phosphate on L-*a*TNA on the T17t template adopted a rigid conformation at the nick site optimal for activation by CNIm,[19] whereas the achiral and flexible SNA cannot fix the phosphate group in a suitable conformation. Thus, helicity and the structural rigidity around phosphate at the nick, both derived from the chirality of the XNA scaffold, are important for highly efficient ligation.

Which is More Important: The Helicity or the Local Conformation of the Phosphate? For further investigation of the effect of chirality, we examined the chemical ligation of L-*a*TNA-SNA chimeric strands (Figure 2). We designed chimera fragments with one, two, or four L-*a*TNA units and evaluated their ligation on the S16t template (Figure 2a, Table S2). All chimeric fragments had higher k_{obs} values than fully SNA fragments, indicative of the positive effect of chirality on ligation. Interestingly, the CD spectrum of T2S6-Alp-S6T2-B/S16t, in which two L-*a*TNA units were present at the termini of each fragment, had almost the same CD spectrum as that of the L-*a*TNA duplex (T8Alp-T8B/T16t) (Figure 2b). This result demonstrates that the right-handed helicity was sufficiently propagated through the duplex by only two L-*a*TNA residues. This was expected based on previous results.[22] Terminal modification of fragments with L-*a*TNA increased the reaction rate compared to SNA fragments, and a single substitution was as effective as four per fragment due to the saturation of helical propagation (Figure 2a, entries 12−14). This is the first demonstration of acceleration of a chemical ligation reaction by remote helical propagation, although helical propagation had been shown to induce chirality-selective incorporation of fragments.[13] Surprisingly, a single substitution of either fragment at the nick position with L-*a*TNA significantly accelerated the reaction, which was obviously superior to multiple substitutions at the termini (Figure 2a, entries 10−11). The rate was further amplified by combining chimeric fragments and chimeric templates T2S12T2-t and S7T2S7-t, compared to their sole use (Figures 2a,d, S7, and Table S2). The k_{obs} for ligation of S7T1-A to p-T1S7-B on the S7T2S7-t template, where L-*a*TNA residues were at the nick site of both fragments and in the complementary positions in the template, was further increased, which was remarkably higher than that for ligation of T2S6-A to p-S6T2-B on T2S8T2-t, even though both duplexes had almost the same right-handed helicities (Figure 2c,d).

Thus, we conclude that the more critical role of chirality in chemical ligation efficiency is to impart rigidity to the phosphate conformation at the nick site and that the induction of helicity is less important.

Further Study on Chirality at the Nick Site Using XNA-SNA Chimeric Fragments. To gain further insights into the effect of chirality at the nick site on the chemical ligation, we also prepared SNA chimeric fragments containing *acyclic* D-threoninol nucleic acid (D-*a*TNA)[23] and *acyclic* L-*allo*-threoninol nucleic acid (L-*allo*-*a*TNA)[24] at the nick site (Figures 3, S8−S10, and Table S2). D-*a*TNA is an enantiomer of L-*a*TNA, and L-*allo*-*a*TNA is a stereoisomer of L-*a*TNA

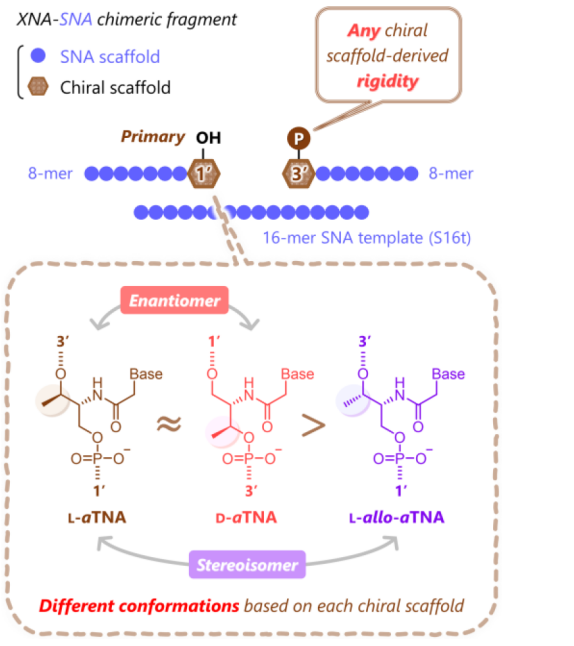

Figure 3. Effects of rigidity/conformation derived from chiral scaffolds (L-*a*TNA, D-*a*TNA, and L-*allo*-*a*TNA) on chemical ligations.

https://doi.org/10.1021/jacs.5c03128
J. Am. Chem. Soc. 2025, 147, 17967−17974

with different chiralities on the carbon tethering methyl group. In both cases, 3′−OH was phosphorylated and reacted with the primary hydroxyl group on another fragment for fair comparison. The result of ligation of these fragments on S16t indicated that the introduction of either a D-*a*TNA or an L-*allo*-*a*TNA into the phosphorylated fragment also increased the ligation rate compared to the SNA fragments (Figure S10; S7DT1-A-p|S8B: k_{obs} = 0.14 h^{-1} and S8Alp-LalloT1S7-B: k_{obs} = 0.12 h^{-1}, respectively). This result is fully consistent with the L-*a*TNA-SNA chimera: chirality-induced rigidity by an additional methyl group accelerated the activation of the phosphate group. In contrast, the substitution of OH termini at the nick site resulted in different effects depending on its chirality. The D-*a*TNA-SNA chimeric fragment also accelerated the reaction (Figure S10; S8A|DT1S7-B: k_{obs} = 0.10 h^{-1}) but was less effective than S7DT1-A-p|S8B, whereas the L-*allo*-*a*TNA-SNA chimeric fragment reduced the reaction rate (Figure S10; S7LalloT1-A|S8B: k_{obs} = 0.073 h^{-1}). The result of the D-*a*TNA-SNA system is consistent with the L-*a*TNA-SNA system because the L-*a*TNA-SNA/SNA duplex is an enantiomer of the D-*a*TNA-SNA/SNA duplex with an inverted sequence. The suppression of the reaction by the L-*allo*-*a*TNA-SNA chimeric fragment implies that the correct chirality of the scaffold tethering nucleophile-OH is important to facilitate the effective ligation. Our previous study on the duplex stability of *allo*-*a*TNA revealed that full-modification with *allo*-*a*TNA is unfavorable to form duplexes,[24] supporting the unsuitability of chirality on *allo*-*a*TNA to be ligated. Interestingly, when both fragments were substituted, the chirality effect was enhanced: the reaction rate of S7DT1-A-p|DT1S7-B further increased (Figure S10; k_{obs} = 0.25 h^{-1}), whereas that of S7LalloT1-Alp-LalloT1S7-B decreased (k_{obs} = 0.042 h^{-1}) compared to single modifications. The dual incorporation of *allo*-*a*TNA presumably induced distortion of the local structure of the nick site of the duplex due to incorrect rigidity, dominantly reducing the reaction rate rather than the acceleration of phosphate activation.

Overall, we confirmed that the chirality of the phosphorylated scaffold at the nick site produced rigidity that enhanced the activation of the phosphate group, irrespective of the stereochemistry of the methyl group, whereas the scaffold tethering nucleophile-OH required correct chirality to facilitate a proper conformation for effective ligation (Figure 3).

Template Composition Study on the Chemical Ligation and Its Application in Nonenzymatic Reverse Transcription from Natural Nucleic Acids to L-*a*TNA. Both L-*a*TNA and SNA form A-form duplexes with complementary DNA and RNA,[14−16] and we expected that DNA and RNA, which have chiral scaffolds, would facilitate effective chemical ligation reactions of the XNAs. Chiral DNA and RNA templates (D17t and R17t, respectively) increased the ligation rates of S8A to p-S8B (k_{obs} = 0.15 and 0.17 h^{-1}, respectively) relative to ligation on the SNA template (k_{obs} = 0.094 h^{-1}) (Figures 4, S2, and S3). Note that the T_ms of SNA/DNA or SNA/RNA heteroduplexes are much lower than those of the SNA/SNA homoduplexes, as shown in previous work.[15,16] Similarly, the use of DNA and RNA templates improved the ligation of L-*a*TNA fragments compared to the SNA template (Figure 4). Besides, this tendency was also observed with longer sequences (Figure S11).

The effective ligation of L-*a*TNA fragments on DNA and RNA templates prompted us to examine the "reverse transcription" reaction of sequence-specific L-*a*TNA synthesis

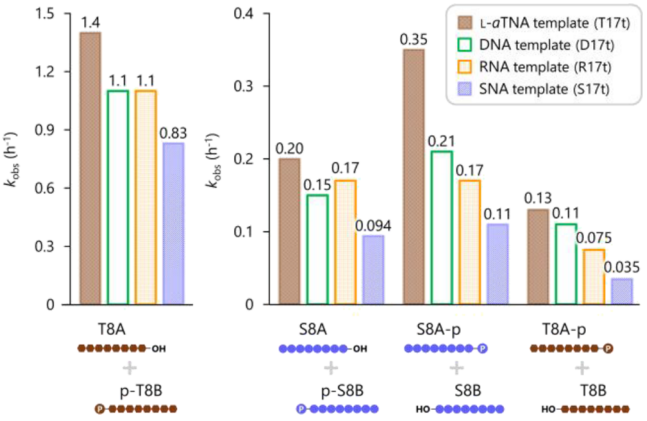

Figure 4. Ligation efficiency (k_{obs}) for indicated fragment pairs on indicated templates in a solution containing Mn^{2+} solution. Reaction conditions: 0.9 μM S8A, S8A-p, T8A, or T8A-p, 1.1 μM p-S8B, S8B, p-T8B, or T8B, 1.0 μM T17t, D17t, R17t, or S17t, 100 mM NaCl, 20 mM $MnCl_2$, 20 mM CNIm, 4 °C.

on natural nucleic acid templates. The chemical primer extension of L-*a*TNA was performed essentially as previously reported.[18,19] Sequential extension of an eight-mer L-*a*TNA primer (T8A) on 17-mer DNA, RNA, or SNA templates was performed in the presence of the three complementary L-*a*TNA trimers, a divalent cation, and CNIm (Figure 5a).

For all templates, T8A was gradually converted to 11-mer and 14-mer intermediates and then full-length 17-mer product (Figures 5b, S12−S14, and Table S4). The identity of the 17-mer full-length product was confirmed by mass spectroscopy (Figures S16 and S17). Interestingly, in the presence of Mn^{2+}, despite the lower binding affinity of L-*a*TNA for DNA and RNA than for L-*a*TNA, the elongation of L-*a*TNA was accomplished on DNA and RNA templates. The rates of elongation were similar on the RNA template and the L-*a*TNA template, whereas the rates were slower on the DNA and SNA templates (Figure 5b). This is in contrast to the results with 8-mer fragments: Ligation was equally effective on DNA and RNA templates for 8-mer fragments. We also examined the elongation kinetics in the presence of Cd^{2+} (Figures 5b, S12, S14−S15, and Table S4). The ligation rates on both the RNA and SNA templates were improved relative to those in Mn^{2+}, whereas the rate on the DNA template remained low (Figure 5b).

The slow reaction on the DNA template likely resulted from the low affinity between L-*a*TNA trimers and the DNA template, which was previously reported.[14,16] Thus, the rate-determining step of the L-*a*TNA/DNA system was the hybridization step that is not significantly influenced by the metal cation identity.[19] This hypothesis was supported by the experiment using tetramer fragments: Ligation on the DNA template proceeded as efficiently with 1 equiv of L-*a*TNA tetramer fragments (Figure S21) as with 50 equiv of trimer fragments (Figure 5b). On the RNA template, ligation was efficient with L-*a*TNA trimers and with tetramers (Figure S22). Importantly, elongation on the RNA template was more rapid than that on the SNA template due to the chiral effect.

Finally, we attempted reverse transcription from RNA to L-*a*TNA in the presence of a pool of the 64 possible L-*a*TNA trimers. The full-length ligation product was obtained in 78% yield after 24 h in the Mn^{2+}/CNIm system (Figure 5c), with its identity confirmed by mass spectroscopy (Figure S23).

https://doi.org/10.1021/jacs.5c03128
J. Am. Chem. Soc. 2025, 147, 17967−17974

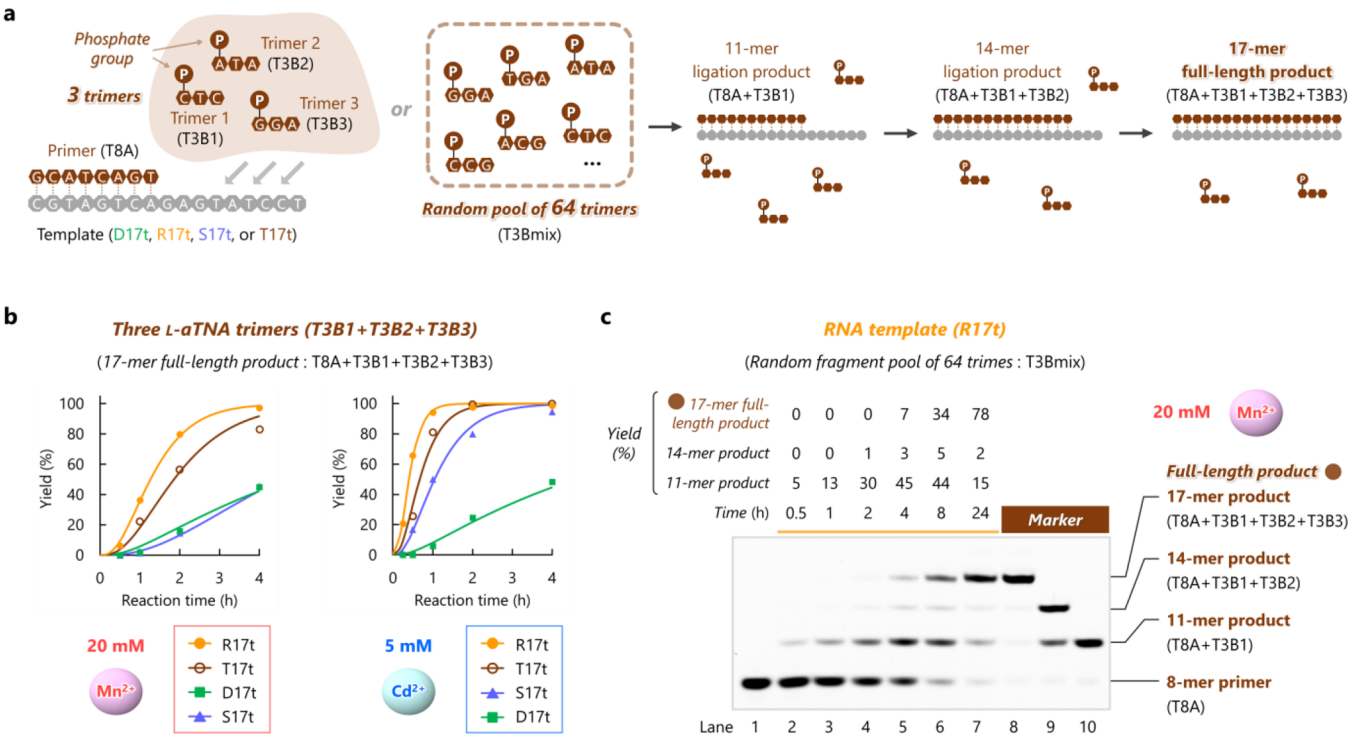

Figure 5. (a) Schematic of nonenzymatic reverse transcription. (b) Percent yield of full-length product on the DNA template (D17t), RNA template (R17t), SNA template (S17t), and L-*a*TNA template (T17t) in solutions containing T3B1, T3B2, and T3B3 and Mn^{2+} or Cd^{2+} as a function of time. Data for T17t in Mn^{2+} is from previous work.[18] Other PAGE analyses are shown in Figures S14 and S15. Reaction conditions: 0.9 μM T8A, 1.0 μM D17t, R17t, S17t, or T17t, 50 μM T3B1, T3B2, and T3B3, 100 mM NaCl, 20 mM $MnCl_2$ or 5 mM $CdCl_2$, 20 mM CNIm, 4 °C. (c) Denaturing PAGE analysis of chemical reverse transcription on an RNA template (R17t) in the presence of a random pool of 64 L-*a*TNA trimers (T3Bmix) and Mn^{2+}. Reaction conditions: 0.9 μM T8A, 1.0 μM R17t, 300 μM T3Bmix, 100 mM NaCl, 20 mM $MnCl_2$, 20 mM CNIm, and 4 °C. PAGE conditions: 20% acrylamide, 8 M urea, 1× TBE, 2 h, 65 °C, 4 W. Negative controls (lane 1) included only T8A, NaCl, and $MnCl_2$. Markers were prepared by the chemical reaction under the same conditions with only the indicated trimers (Figures S14 and S18–S20).

Unfortunately, we have no methodology for direct sequencing of L-*a*TNA at present, and identification is limited to the mass. The yield was comparable to that reported previously on an L-*a*TNA template (>75% yield, 24 h).[18] The reverse transcription reaction was accelerated by Cd^{2+}; however, the final yield of the full-length product was slightly lower than that in Mn^{2+} (Figures 5b and S24). Since the L-*a*TNA/RNA duplex was less stable than L-*a*TNA/L-*a*TNA, the hybridization step of the trimers would be more critical for L-*a*TNA elongation on the RNA template. Cd^{2+} possibly suppressed the hybridization of the trimers because Cd^{2+} does not stabilize the duplex between RNA and L-*a*TNA as effectively as Mn^{2+} does.[19]

Reverse transcription from SNA to L-*a*TNA was detected in the presence of the L-*a*TNA trimer pool; however, the yield was lower than that on the RNA template: 63% at 24 h in the Mn^{2+}/CNIm system (Figures S25 and S26), demonstrating the importance of chirality for strand elongation. On the DNA template, only the 11-mer product was detected, and yields were low in the presence of the L-*a*TNA trimer pool (Figure S27). Even with a 4-mer L-*a*TNA fragment pool, the yields of reverse transcription from the DNA template were low (Figure S28). The reverse transcription from DNA to L-*a*TNA would be facilitated by stabilization of the duplex using additives such as trimethylamine *N*-oxide, a cationic comb-type copolymer (poly(L-lysine)-*graft*-dextran), groove binders, and so on.[25]

CONCLUSIONS

The chemical structure of SNA is very similar to that of L-*a*TNA; the only difference is the absence of a methyl group in the main chain of SNA. The melting temperature of an SNA homoduplex is similar to that of an L-*a*TNA homoduplex of the same sequence; however, the efficiency of the chemical ligation varied considerably. Chemical ligation of complementary fragments on the achiral SNA scaffold was much slower than that on the chiral L-*a*TNA scaffold. The chirality of L-*a*TNA accelerated the chemical ligation mainly by the fixation of the local structure of the phosphate into a conformation suitable for ligation,[26] although helical propagation was also important.[27] The enhancement of the chemical ligation by the chirality enabled effective L-*a*TNA ligation on templates composed of natural nucleic acids. Szostak's group has already made significant contributions to understanding the relationship between rigidity/conformation and nonenzymatic template-directed synthesis using a variety of nucleic acids with ribose backbones.[28] We focused on two similar *acyclic* artificial nucleic acids: SNA with an achiral scaffold and L-*a*TNA with a chiral scaffold. The difference is only the methyl group, which minimizes effects other than chirality in the ligation study. Moreover, most well-studied chemical ligation systems have used preactivated phosphate as substrates, resulting in the rate-determining step being nucleophilic attack and/or the hybridization process. In the case of the CNIm/M^{2+} system used here, the rate-determining factor is the activation of the phosphate group. The different

https://doi.org/10.1021/jacs.5c03128
J. Am. Chem. Soc. 2025, 147, 17967−17974

pathways from previous research provided findings that offer novel perspectives following pioneering works.

These data suggest that genomic information encoded by chiral carriers is more efficiently replicated than that encoded by achiral carriers, which is valuable insight for XNA-based systems and may be applicable to natural systems. We also demonstrated reverse transcription from RNA to L-*a*TNA using all possible L-*a*TNA trimers as ingredients. Once transcription from L-*a*TNA to natural nucleic acid is achieved, L-*a*TNA-based in vitro selection and an artificial life system, including nonenzymatic translation, will become possible.

■ ASSOCIATED CONTENT

Supporting Information

The Supporting Information is available free of charge at https://pubs.acs.org/doi/10.1021/jacs.5c03128.

Experimental details for preparation of experimental materials, sequences, pH measurements, melting temperatures, and additional figures and tables (PDF)

■ AUTHOR INFORMATION

Corresponding Authors

Keiji Murayama − *Graduate School of Engineering, Nagoya University, Nagoya 464-8603, Japan;* orcid.org/0000-0002-6537-0120; Email: murayama@chembio.nagoya-u.ac.jp

Hiroyuki Asanuma − *Graduate School of Engineering, Nagoya University, Nagoya 464-8603, Japan;* orcid.org/0000-0001-9903-7847; Email: asanuma@chembio.nagoya-u.ac.jp

Author

Hikari Okita − *Graduate School of Engineering, Nagoya University, Nagoya 464-8603, Japan;* orcid.org/0009-0006-0168-5584

Complete contact information is available at: https://pubs.acs.org/10.1021/jacs.5c03128

Notes

The authors declare no competing financial interest.

■ ACKNOWLEDGMENTS

This work was supported by the JST ACT-X (JPMJAX2325 to H.O.), JST FOREST Program (JPMJFR2226 to K.M.), JSPS KAKENHI grants Grant-in-Aid for Transformative Research Areas "Molecular Cybernetics" (JP20H05970 and JP20H05968 to K.M.), JSPS Grant-in-Aid for Scientific Research (S) (JP21H05025 to H.A.), and AMED (23am0401007 and 24ae0121056 to H.A.).

■ REFERENCES

(1) (a) Bhowmik, S.; Krishnamurthy, R. The Role of Sugar-Backbone Heterogeneity and Chimeras in the Simultaneous Emergence of RNA and DNA. *Nat. Chem.* **2019**, *11* (11), 1009−1018. (b) Kim, S. C.; Zhou, L.; Zhang, W.; O'Flaherty, D. K.; Rondo-Brovetto, V.; Szostak, J. W. A Model for the Emergence of RNA from a Prebiotically Plausible Mixture of Ribonucleotides, Arabinonucleotides, and 2'-Deoxynucleotides. *J. Am. Chem. Soc.* **2020**, *142* (5), 2317−2326.

(2) (a) Joshi, P. C.; Pitsch, S.; Ferris, J. P. Selectivity of Montmorillonite Catalyzed Prebiotic Reactions of D, L-Nucleotides. *Orig. Life Evol. Biosph.* **2007**, *37*, 3−26. (b) Bonner, W. A. Chirality and Life. *Orig Life Evol Biosph.* **1995**, *25*, 175−190. (c) Blackmond, D. G. The Origin of Biological Homochirality. *Cold Spring Harb Perspect Biol.* **2010**, *2* (5), No. a002147.

(3) (a) Dreiling, J. M.; Gay, T. J. Chirally Sensitive Electron-Induced Molecular Breakup and the Vester-Ulbricht Hypothesis. *Phys. Rev. Lett.* **2014**, *113* (11), No. 118103. (b) Ulbricht, T. L.; Vester, F. Vester Attempts to induce optical activity with polarized *β*-radiation. *Tetrahedron* **1962**, *18*, 629−637. (c) Ulbricht, T. L. V. The Origin of Optical Asymmetry on Earth. *Origins of Life* **1975**, *6*, 303−315. (d) Bonner, W. A. Parity Violation and the Evolution of Biomolecular Homochirality. *Chirality* **2000**, *12*, 114−126. (e) Chen, Y.; Ma, W. The Origin of Biological Homochirality along with the Origin of Life. *PLoS Comput. Biol.* **2020**, *16* (1), No. e1007592.

(4) (a) Weimann, B. J.; Lohrmann, R.; Orgel, L. E.; Schneider-Bernloehr, H.; Sulston, J. E. Template-Directed Synthesis with Adenosine-5′-Phosphorimidazolide. *Science* **1968**, *161* (3839), 387. (b) Chaput, J. C.; Switzer, C. Nonenzymatic Oligomerization on Templates Containing Phosphodiester-Linked Acyclic Glycerol Nucleic Acid Analogues. *J. Mol. Evol.* **2000**, *51* (5), 464−470. (c) Mansy, S. S.; Schrum, J. P.; Krishnamurthy, M.; Tobé, S.; Treco, D. A.; Szostak, J. W. Template-Directed Synthesis of a Genetic Polymer in a Model Protocell. *Nature* **2008**, *454* (7200), 122−125. (d) Deck, C.; Jauker, M.; Richert, C. Efficient Enzyme-Free Copying of All Four Nucleobases Templated by Immobilized RNA. *Nat. Chem.* **2011**, *3* (8), 603−608. (e) Attwater, J.; Raguram, A.; Morgunov, A. S.; Gianni, E.; Holliger, P. Ribozyme-Catalysed RNA Synthesis Using Triplet Building Blocks. *eLife* **2018**, *7*, No. e35255. (f) Obianyor, C.; Newnam, G.; Clifton, B. E.; Grover, M. A.; Hud, N. V. Towards Efficient Nonenzymatic DNA Ligation: Comparing Key Parameters for Maximizing Ligation Rates and Yields with Carbodiimide Activation. *ChemBioChem.* **2020**, *21* (23), 3359−3370. (g) Leveau, G.; Pfeffer, D.; Altaner, B.; Kervio, E.; Welsch, F.; Gerland, U.; Richert, C. Enzyme-Free Copying of 12 Bases of RNA with Dinucleotides. *Angew. Chem., Int. Ed.* **2022**, *61* (29), No. e202203067. (h) Mizuuchi, R.; Ichihashi, N. Minimal RNA Self-Reproduction Discovered from a Random Pool of Oligomers. *Chem. Sci.* **2023**, *14* (28), 7656−7664. (i) Fang, Z.; Pazienza, L. T.; Zhang, J.; Tam, C. P.; Szostak, J. W. Catalytic Metal Ion−Substrate Coordination during Nonenzymatic RNA Primer Extension. *J. Am. Chem. Soc.* **2024**, *146* (15), 10632−10639. (j) Serrão, A. C.; Wunnava, S.; Dass, A. V.; Ufer, L.; Schwintek, P.; Mast, C. B.; Braun, D. High-Fidelity RNA Copying via 2',3′-Cyclic Phosphate Ligation. *J. Am. Chem. Soc.* **2024**, *146* (13), 8887−8894.

(5) (a) Joyce, G. F.; Inoue, T.; Orgel, L. E. Non-enzymatic template-directed synthesis on RNA random copolymers: Poly(C, U) templates. *J. Mol. Biol.* **1984**, *176* (2), 279−306. (b) Walton, T.; Szostak, J. W. A Highly Reactive Imidazolium-Bridged Dinucleotide Intermediate in Nonenzymatic RNA Primer Extension. *J. Am. Chem. Soc.* **2016**, *138* (36), 11996−12002. (c) Zhou, L.; O'Flaherty, D. K.; Szostak, J. W. Template-Directed Copying of RNA by Non-enzymatic Ligation. *Angew. Chem., Int. Ed. Engl.* **2020**, *59* (36), 15682−15687. (d) Welsch, F.; Kervio, E.; Tremmel, P.; Richert, C. Prolinyl Nucleotides Drive Enzyme-Free Genetic Copying of RNA. *Angew. Chem., Int. Ed. Engl.* **2023**, *62* (41), No. e202307591.

(6) (a) Joyce, G. F.; Vissert, G. M.; van Boeckel, C. A. A.; van Boomt, J. H.; Orgel, L. E.; van Westrenent, J. Chiral Selection in Poly(C)-Directed Synthesis of Oligo(G). *Nature* **1984**, *310* (5978), 602−604. (b) Bolli, M.; Micural, R.; Eschenmoser, A. Pyranosyl-RNA: Chiroselective Self-Assembly of Base Sequences by Ligative Oligomerization of Tetranucleotide-2',3′-Cyclophosphates (with a Commentary Concerning the Origin of Biomolecular Homochirality). *Chem. Biol.* **1997**, *4* (4), 309−320. (c) Kozlov, I. A.; Pitsch, S.; Orgel, L. E. Oligomerization of Activated D- and L-Guanosine Mononucleotides on Templates Containing D- and L-Deoxycytidylate Residues. *Proc. Natl. Acad. Sci. U.S.A.* **1998**, *95* (23), 13448−13452. (d) Tjhung, K. F.; Sczepanski, J. T.; Murtfeldt, E. R.; Joyce, G. F. RNA-Catalyzed Cross-Chiral Polymerization of RNA. *J. Am. Chem. Soc.* **2020**, *142* (36), 15331−15339. (e) Mangalath, S.; Karunakaran, S. C.; Newnam, G.; Schuster, G. B.; Hud, N. V. Supramolecular

Assembly-Enabled Homochiral Polymerization of Short $(dA)_n$ Oligonucleotides. *Chem. Commun.* **2021**, *57*, 13602.
(7) (a) Joyce, G. F.; Schwartz, A. W.; Miller, S. L.; Orgel, L. E. The case for an ancestral genetic system involving simple analogues of the nucleotides. *Proc. Natl. Acad. Sci. U.S.A.* **1987**, *84* (13), 4398−4402. (b) Schneider, K. C.; Benner, S. A. Oligonucleotides Containing Flexible Nucleoside Analogs. *J. Am. Chem. Soc.* **1990**, *112* (1), 453−455. (c) Merle, L.; Spach, G.; Merle, Y.; Sági, J.; Szemzö, A. Some biochemical properties of an acyclic oligonucleotide analogue. A plausible ancestor of the DNA? *Orig. Life Evol. Biosph.* **1993**, *23*, 91−103.
(8) (a) Nielsen, P. E.; Egholm, M.; Berg, R. H.; Buchardt, O. Sequence-Selective Recognition of DNA by Strand Displacement with a Thymine-Substituted Polyamide. *Science* **1991**, *254* (5037), 1497−1500. (b) Egholm, M.; Buchardt, O.; Christensen, L.; Behrens, C.; Freler, S. M.; Driver, D. A.; Bergt, R. H.; Kim, S. K.; Norden, B.; Nielsen, P. E. PNA Hybridizes to Complementary Oligonucleotides Obeying the Watson-Crick Hydrogen-Bonding Rules. *Nature* **1993**, *365* (6446), 566−568.
(9) (a) Bohler, C.; Nielsen, P. E.; Orgel, L. E. Template Switching between PNA and RNA Oligonucleotides. *Nature* **1995**, *376* (6541), 578−581. (b) Schmidt, J. G.; Christensen, L.; Nielsen, P. E.; Orgel, L. E. Information Transfer from DNA to Peptide Nucleic Acids by Template-Directed Syntheses. *Nucleic Acids Res.* **1997**, *25* (23), 4792−4796. (c) Schmidt, J. G.; Nielsen, P. E.; Orgel, L. E. Information Transfer from Peptide Nucleic Acids to RNA by Template-Directed Syntheses. *Nucleic Acids Res.* **1997**, *25* (23), 4797−4802.
(10) (a) Rosenbaum, D. M.; Liu, D. R. Efficient and Sequence-Specific DNA-Templated Polymerization of Peptide Nucleic Acid Aldehydes. *J. Am. Chem. Soc.* **2003**, *125* (46), 13924−13925. (b) Brudno, Y.; Birnbaum, M. E.; Kleiner, R. E.; Liu, D. R. An In Vitro Translation, Selection, and Amplification System for Peptide Nucleic Acids. *Nat. Chem. Biol.* **2010**, *6* (2), 148−155.
(11) (a) Singhal, A.; Nielsen, P. E. Cross-Catalytic Peptide Nucleic Acid (PNA) Replication Based on Templated Ligation. *Org. Biomol. Chem.* **2014**, *12*, 6901−6907. (b) Plöger, T. A.; von Kiedrowski, G. A Self-Replicating Peptide Nucleic Acid. *Org. Biomol. Chem.* **2014**, *12*, 6908−6914. (c) Heemstra, J. M.; Liu, D. R. Templated Synthesis of Peptide Nucleic Acids via Sequence-Selective Base-Filling Reactions. *J. Am. Chem. Soc.* **2009**, *131* (32), 11347−11349. (d) Michaelis, J.; Roloff, A.; Seitz, O. Amplification by Nucleic Acid-Templated Reactions. *Org. Biomol. Chem.* **2014**, *12*, 2821−2833.
(12) Joshi, S.; Romanens, P.; Winssinger, N. Sequencing of D/L-DNA and XNA by Templated-Synthesis. *J. Am. Chem. Soc.* **2025**, *147*, 6288.
(13) Kozlov, I. A.; Orgel, L. E.; Nielsen, P. E. Remote Enantioselection Transmitted by an Achiral Peptide Nucleic Acid Backbone. *Angew. Chem., Int. Ed.* **2000**, *39* (23), 4292−4295.
(14) Murayama, K.; Kashida, H.; Asanuma, H. *Acyclic* L-Threoninol Nucleic Acid (L-*a*TNA) with Suitable Structural Rigidity Cross-Pairs with DNA and RNA. *Chem. Commun.* **2015**, *51* (30), 6500−6503.
(15) Kashida, H.; Murayama, K.; Toda, T.; Asanuma, H. Control of the Chirality and Helicity of Oligomers of Serinol Nucleic Acid (SNA) by Sequence Design. *Angew. Chem., Int. Ed.* **2011**, *50*, 1285−1288.
(16) Asanuma, H.; Kamiya, Y.; Kashida, H.; Murayama, K. Xeno Nucleic Acids (XNAs) Having Non-Ribose Scaffolds with Unique Supramolecular Properties. *Chem. Commun.* **2022**, *58* (25), 3993−4004.
(17) Chen, Y.; Nagao, R.; Murayama, K.; Asanuma, H. Orthogonal Amplification Circuits Composed of Acyclic Nucleic Acids Enable RNA Detection. *J. Am. Chem. Soc.* **2022**, *144* (13), 5887−5892.
(18) Murayama, K.; Okita, H.; Kuriki, T.; Asanuma, H. Non-enzymatic Polymerase-Like Template-Directed Synthesis of Acyclic L-threoninol Nucleic Acid. *Nat. Commun.* **2021**, *12* (1), 804.
(19) Okita, H.; Kondo, S.; Murayama, K.; Asanuma, H. Rapid Chemical Ligation of DNA and *Acyclic* Threoninol Nucleic Acid (*a*TNA) for Effective Nonenzymatic Primer Extension. *J. Am. Chem. Soc.* **2023**, *145*, 17872−17880.
(20) (a) Liu, Z.; Jiang, C. Z.; Bond, A. D.; Tosca, N. J.; Sutherland, J. D. Manganese(ii) Promotes Prebiotically Plausible Non-Enzymatic RNA Ligation Reactions. *Chem. Commun.* **2024**, *60* (51), 6528−6531. (b) Kanaya, E.; Yanagawa, H. Template-Directed Polymerization of Oligoadenylates Using Cyanogen Bromide. *Biochemistry* **1986**, *25* (23), 7423−7430.
(21) (a) Ashley, G. W.; Kushlan, D. M. Chemical Synthesis of Oligodeoxynucleotide Dumbbells. *Biochemistry* **1991**, *30*, 2927−2933. (b) Dolinnaya, N. G.; Sokolova, N. I.; Gryaznova, O. I.; Shabarova, Z. A. Site-Directed Modification of DNA Duplexes by Chemical Ligation. *Nucleic Acids Res.* **1988**, *16* (9), 3721−3738. (c) Dolinnaya, N. G.; Sokolova, N. I.; Ashirbekova, D. T.; Shabarova, Z. A. The Use of BrCN for Assembling Modified DNA Duplexes and DNA-RNA Hybrids; Comparison with Water-Soluble Carbodiimide. *Nucleic Acids Res.* **1991**, *19* (11), 3067−3072.
(22) Kashida, H.; Nishikawa, K.; Shi, W.; Miyagawa, T.; Yamashita, H.; Abe, M.; Asanuma, H. A Helical Amplification System Composed of Artificial Nucleic Acids. *Chem. Sci.* **2021**, *12* (5), 1656−1660.
(23) Asanuma, H.; Toda, T.; Murayama, K.; Liang, X.; Kashida, H. Unexpectedly Stable Artificial Duplex from Flexible Acyclic Threoninol. *J. Am. Chem. Soc.* **2010**, *132* (42), 14702−14703.
(24) Murayama, K.; Kashida, H.; Asanuma, H. Methyl group configuration on acyclic threoninol nucleic acids (*a*TNAs) impacts supramolecular properties. *Org. Biomol. Chem.* **2022**, *20* (20), 4115−4122.
(25) (a) Ueda, Y.; Zouzumi, Y.; Maruyama, A.; Nakano, S.; Sugimoto, N.; Miyoshi, D. Effects of Trimethylamine *N*-oxide and Urea on DNA Duplex and G-Guadruplex. *Sci. Technol. Adv. Mater.* **2016**, *17* (1), 753−759. (b) Maruyama, A.; Watanabe, H.; Ferdous, A.; Katoh, M.; Ishihara, T.; Akaike, T. Characterization of Interpolyelectrolyte Complexes between Double-Stranded DNA and Polylysine Comb-Type Copolymers Having Hydrophilic Side Chains. *Bioconjugate Chem.* **1998**, *9* (2), 292−299. (c) Bhaduri, S.; Ranjan, N.; Arya, D. P. An Overview of Recent Advances in Duplex DNA Recognition by Small Molecules. *Beilstein J. Org. Chem.* **2018**, *14*, 1051−1086.
(26) Dolinnaya, N. G.; Tsytovich, A. V.; Sergeev, V. N.; Oretskaya, T. S.; Shabarova, Z. A. Structural and Kinetic Aspects of Chemical Reactions in DNA Duplexes. Information on DNA Local Structure Obtained from Chemical Ligation Data. *Nucleic Acids Res.* **1991**, *19* (11), 3073−3080.
(27) Park, S. J.; Callaghan, K. L.; Ellis, A. V. Role of Helicity in the Nonenzymatic Template-Directed Primer Extension of DNA. *Org. Biomol. Chem.* **2023**, *21* (33), 6702−6706.
(28) (a) Giurgiu, C.; Fang, Z.; Aitken, H. R. M.; Kim, S. C.; Pazienza, L.; Mittal, S.; Szostak, J. W. Structure-Activity Relationships in Nonenzymatic Template-Directed RNA Synthesis. *Angew. Chem., Int. Ed. Engl.* **2021**, *60* (42), 22925−22932. (b) Ding, D.; Zhou, L.; Giurgiu, C.; Szostak, J. W. Kinetic explanations for the sequence biases observed in the nonenzymatic copying of RNA templates. *Nucleic Acids Res.* **2022**, *50* (1), 35−45.

https://doi.org/10.1021/jacs.5c03128
J. Am. Chem. Soc. 2025, 147, 17967−17974